Steel and Composite Structures, *Vol. 35, No. 2 (2020) 199-213*
DOI: https://doi.org/10.12989/scs.2020.35.2.199

Simplified robustness assessment of steel framed structures under fire-induced column failure

Binhui Jiang[1,2a], Guo-Qiang Li[*3,4] and Michael C.H. Yam[2b]

[1]School of Civil Engineering, Central South University, 68 South Shaoshan Road, Changsha 410075, China
[2]Department of Building and Real Estate, The Hong Kong Polytechnic University, Hong Kong, China
[3]College of Civil Engineering, Tongji University, 1239 Siping Road, Shanghai 200092, China
[4]State Key Laboratory for Disaster Reduction in Civil Engineering, Tongji University, Shanghai 200092, China

(*Received July 30, 2019, Revised February 28, 2020, Accepted March 5, 2020*)

Abstract. This paper proposes a Global-Local Analysis Method (GLAM) to assess the progressive collapse of steel framed structures under fire-induced column failure. GLAM obtains the overall structural response by combining dynamic analysis of the heated column (local) with static analysis of the overall structure (global). Test results of two steel frames which explicitly consider the dynamic effect during fire-induced column failure were employed to validate the proposed GLAM. Results show that GLAM gives reasonable predictions to the test frames in terms of both whether to collapse and the displacement verse temperature curves. Besides, several case studies of a two-dimensional (2D) steel frame and a three-dimensional (3D) steel frame with concrete slabs were conducted by using GLAM. Results show that GLAM gives the same collapse predictions to the studied cases with nonlinear dynamic analysis of the whole structure model. Compared with nonlinear dynamic analysis of the whole structure model, GLAM saves approximately 70% and 99% CPU time for the cases of 2D and 3D steel frame, respectively. Results also show that the load level of a structure has notable effects on the restraint condition of a heated column in the structure.

Keywords: steel framed structure; progressive collapse; robustness assessment method; fire-induced column failure; dynamic effect

1. Introduction

The progressive collapse of Ronan Point apartment in 1968 initiated the research on the robustness of structures (Marjanishvili 2004, Pearson and Delatte 2005). Structural robustness refers to the ability of a structure to sustain localized damages caused by abnormal actions without suffering progressive collapse. The abnormal actions could be explosion, impact, fire, consequences of human error, etc. However, research during the following decades was mainly focused on the robustness of structures under explosion or impact, with few research studies of structural robustness under fire. The collapse of the World Trade Center (WTC) towers in 2001 (Lew *et al*. 2005) not only put the research study on structural robustness to a high tide (Ellingwood and Dusenberry 2005, Kim and Park 2008, El-Tawil *et al.* 2014, Mashhadi and Saffari 2017, Ferraioli 2019) but also emphasized the importance of the robustness of structures under fire, because research has shown that it was the fire, instead of the initial damage induced by the airplane impact, that caused the final collapse of these skyscrapers (Usmani *et al.* 2003, Lew *et al.* 2005).

The robustness of building structures under fire has its unique characteristics compared with structural robustness under explosion or impact. Firstly, initial damages caused by explosion or impact usually occur instantaneously, accompanied with severe dynamic effects (Grierson *et al*. 2005, Sasani and Kropelnicki 2008), while the failure process of the heated structural components under fire may be static or dynamic depending on the conditions such as restraint stiffness and load level (Jiang *et al.* 2016). This dynamic effect is mainly due to column buckling. Fang *et al*. (2011) and Jiang *et al*. (2018) show that ignoring the dynamic effect during column buckling may notably underestimate the largest deflection of the structure. Besides, failed components caused by explosion or impact are usually assumed to be totally removed while the heated components under fire usually remain on site, just losing part of their strengths. Therefore, the current structural robustness assessments of buildings concerning with explosion or impact are not applicable to the case of fire.

Significant efforts have been made on the research of robustness of structures under fire during the past two decades (Renaud *et al.* 2003, Wald *et al.* 2006, Kwon and Kwon 2012, Agarwal and Varma 2014, Rackauskaite *et al*. 2017). Lange *et al.* (2012) studied the collapse mechanisms of structures alike the WTC towers under multi-floor fire and proposed a robustness assessment method based on the found mechanisms. However, the proposed method is a static method, without considering the dynamic effects of

∗Corresponding author, Professor
E-mail: gqli@mail.tongji.edu.cn
[a] Ph.D., Lecturer
E-mail: binhuijiang@csu.edu.cn
[b] Ph.D., Professor
E-mail: bsmyam@polyu.edu.hk

ISSN: 1229-9367 (Print), 1598-6233 (Online)

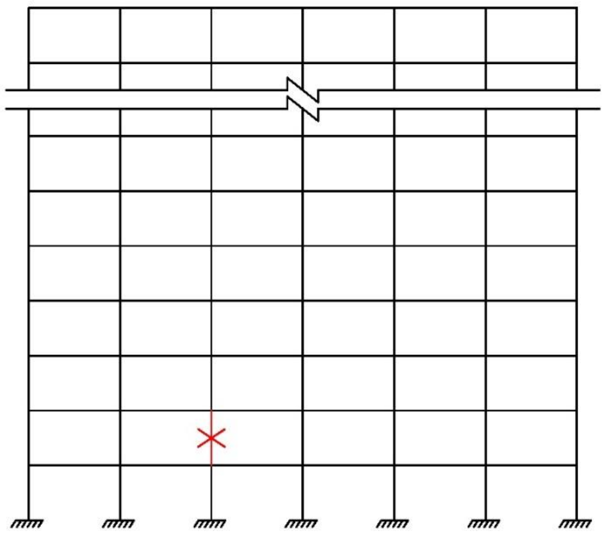

Fig. 1 Illustration of a steel frame with one column fails in fire

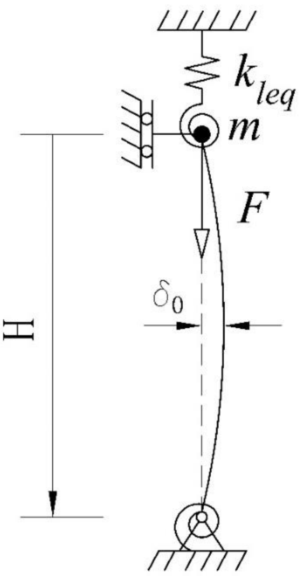

Fig. 2 Model of the heated column

structural performance under fire due to buckling. Sun *et al*. (2012) studied the performance of steel structures under localized fire using dynamic analyses of the whole structure model. Jiang *et al.* (2015, 2017, 2018) summarized three progressive collapse modes of steel frames when one column failed under fire and studied the dynamic effects of steel column buckling under fire through dynamic analyses and experimental studies. Fang *et al.* (2013) proposed an energy-based robustness assessment method, based on an energy-based multi-level assessment framework proposed by Izzuddin *et al*. (2008), on the progressive collapse of multi-storey composite frame buildings under fire. This method does not require the dynamic analysis of the whole structure under localized fire, which significantly reduces the computing cost. However, this method does not consider the strain rate effect of materials which can be significant in those cases where sudden buckling occurs (Jiang *et al.* 2017). Therefore, there is a demand of more alternative performance-based robustness assessment methods of building structures under fire-induced initial failure.

In this paper, a Global-Local Analysis Method, referred to as GLAM hereafter, is proposed to assess the progressive collapse of multi-storey steel framed structures under fire-induced column failure. When one column in a steel framed structure is heated, the structure could be divided into to two parts, namely the heated column, and the unheated sub-structure which is the global structure excluding the heated column. The basic idea of GLAM is to obtain the largest structural displacements through nonlinear dynamic analysis of the heated column, while the boundary condition of the heated column is obtained from nonlinear static analysis of the unheated sub-structure model. Hence, the possible dynamic effects during column buckling, such as

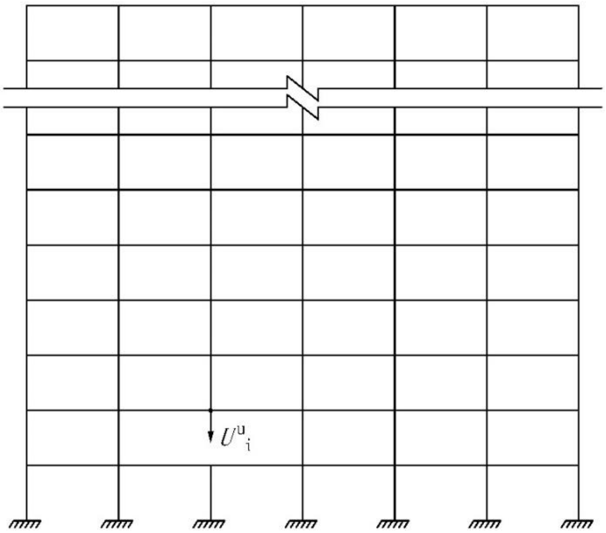

Fig. 3 Illustration of the unheated sub-structure after excluding the heated components

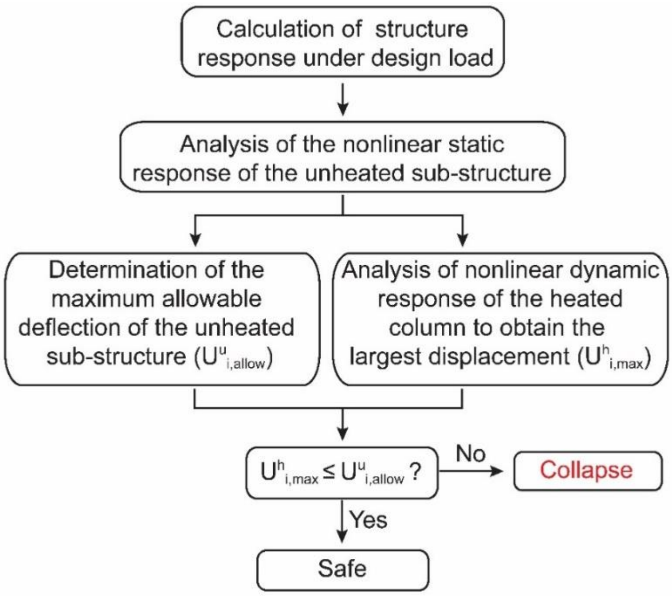

Fig. 4 Assessment procedure of the proposed robustness assessment method (GLAM)

strain rate effect of material and inertial effect, are considered by GLAM. The proposed GLAM was validated by experimental results of two tested steel frames reported in (Jiang *et al.* 2018). Several case studies of a 2D steel frame and a 3D steel frame with concrete slabs are also adopted to demonstrate the application of GLAM. Finally, some key issues in application of GLAM is discussed.

2. Assessment procedure of GLAM

The GLAM is aimed at offering a feasible and simplified method to assess the progressive collapse of steel framed structures under fire-induced column failure as illustrated in Fig. 1. This applies to the scenario that a localized fire occurs near a steel column where the composite floor is considered to remain at ambient temperature due to the thermal isolation of the ceilings (Jiang and Li 2017). When one column in a steel framed structure is heated, the response of the structure typically involves significant geometric and material nonlinearity, some cases may also involve significant dynamic effects (Jiang *et al.* 2018). Although the most accurate way to assess the progressive collapse of a building structure under this scenario is through nonlinear dynamic analysis of the whole structure, which is normally time-consuming. A more practical assessment method entitled GLAM is proposed here which is computationally efficient, yet effective. The GLAM obtains the largest structural response by nonlinear dynamic analysis of the heated column, as shown in Fig. 2. The boundary restraint conditions of the heated column model and the collapse criterion of the structure is obtained through nonlinear static analysis of the unheated sub-structure, as illustrated in Fig. 3. The flowchart of assessment procedure of the GLAM is shown in Fig. 4. As shown in Fig. 4, the GLAM contains five steps as follows:

(1) calculation of response of the structure under design load;

(2) analysis of the nonlinear static response of the unheated sub-structure;

(3) determination of the maximum allowable deflection of the unheated sub-structure;

(4) analysis of nonlinear dynamic response of the heated column;

(5) assessment of progressive collapse by comparing the maximum response of the heated column with the maximum allowable deflection of the unheated sub-structure.

These steps are described in detail in the following subsections.

2.1 Response of the structure under design load

The objective of this step is to obtain the node displacements and internal forces of the heated column in the structure at ambient temperature under design load (Fig. 1). Since the structure of a multi-storey steel building is usually in elastic state under design load, the structural response could be easily obtained through linear static finite element analysis or structural mechanics method.

2.2 Nonlinear static response of the unheated sub-structure

The unheated sub-structure as shown in Fig. 3 offers restraints to the heated column. This step is to analyse the boundary restraints offered by the unheated sub-structure to the heated column. When analysing the restraint along a degree freedom (U_i^u) at one node, the displacement of the considered degree of freedom at this node is first restrained. Secondly, the designed vertical load is applied to the unheated sub-structure. Finally, the displacement (U_i^u) is gradually applied to this node as illustrated in Fig. 3. The reaction force (Q_i^u) along the same direction of U_i^u at this node then could be obtained by nonlinear static analysis. Since in robustness assessment, the structure is allowed to undergo large deflection and material plasticity as long as it will not collapse, both material nonlinearity and geometric nonlinearity should be considered in the analysis of this step. The restraints offered by the unheated sub-structure to the heated components at this node could then be represented by the corresponding reaction-displacement (Q_i^u-U_i^u) curve. Considering that the bottom point of the heated column in the whole structure will undergo some displacement along the considered degree of freedom (U_i^0) when the design load is applied to the structure, as introduced in subsection 2.1, the zero point of the displacement axis of the reaction-displacement curve should be adjusted to the position of (U_i^0). The tangent stiffness of this restraint spring (K_i^u) could be obtained from the reaction-displacement (Q_i^u-U_i^u) curve.

2.3 Maximum allowable deflection of the unheated sub-structure

The maximum allowable deflection ($U_{i,allow}^u$) of the unheated sub-structure could be determined based on the responses of the unheated sub-structure obtained in step (2). The maximum allowable deflection could be adopted as the minimum value of the following deflections: deflection at which composite floors in the unheated sub-structure fail ($U_{i,allow1}^u$), deflection when unheated columns buckle ($U_{i,allow2}^u$), or the maximum deflection that the owner allows ($U_{i,allow3}^u$), as shown in the following equation

$$U_{i,allow}^u = \min(U_{i,allow1}^u, U_{i,allow2}^u, U_{i,allow3}^u) \qquad (1)$$

2.4 Nonlinear dynamic analysis of the heated column

A simplified analysis model of the heated column is constructed as shown in Fig. 2. The nonlinear dynamic response of the heated column under fire is examined using the simplified model. The restraints offered by the unheated sub-structure are modelled using springs, and the reaction-displacement curves of the spring elements are adopted from the corresponding reaction-displacement curves obtained in step (2). Load is applied to the heated column so that its internal force is the same as that under design load. Besides, the corresponding mass of the applied force was attached to the top point of the column to consider the inertial effects in dynamic analysis.

As mentioned in the Introduction section, sever dynamic effects may appear to the structure during column buckling under thermal loading. A nonlinear dynamic analysis, which considers the strain rate effects of material and inertial effect, is conducted to learn the performance of the sub-structure under thermal loading. The dynamic equilibrium equation of the heated column is as follow

$$M^h\ddot{U}^h(t) + C^h\dot{U}^h(t) + K^hU^h(t) = Q^h(t) \qquad (2)$$

where M^h, C^h and K^h are mass matrix, damping matrix and stiffness matrix of the heated column, respectively; $\ddot{U}^h(t)$, $\dot{U}^h(t)$ and $U^h(t)$ are the acceleration vector, velocity vector and displacement vector of the heated column, respectively; and $Q^h(t)$ is the external load vector of the heated column. However, research in (Jiang *et al.* 2017) shows that for steel structures under fire, the effect of damping is negligible. Through the above nonlinear dynamic analysis, the maximum displacement of the heated column $U_{i,max}^h$ could be obtained.

The duration of the thermal loading process of a building structure in fire could be from minutes to hours, and adopting the real time for such a process in a dynamic analysis is time-consuming. Research studies (Jiang *et al.* 2015, Jiang *et al.* 2017) show that in the dynamic analysis of a structure that suffers thermal loading, the thermal loading process could be scaled to seconds by using time scale technique in order to save computational cost. However, a sensitivity analysis should be conducted to determine the appropriate time duration.

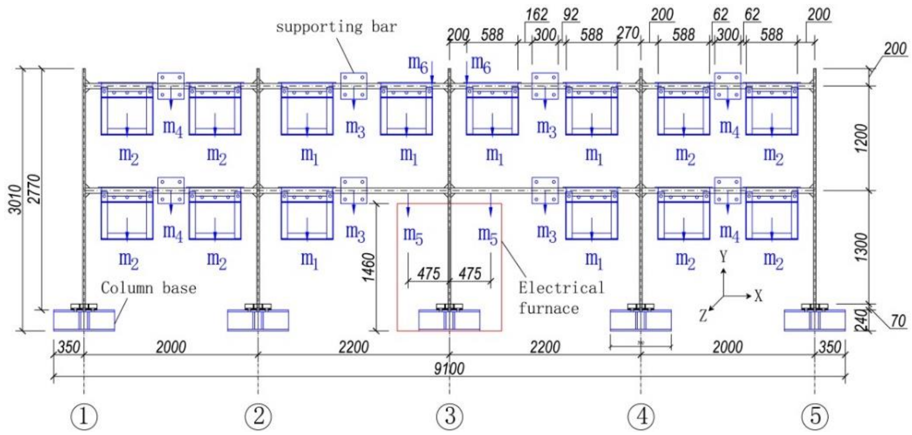

Fig. 5 Tested steel frame in localized thermal loading (Jiang *et al.* 2018)

Table 1 Member sections of the test frames (Dimensions in mm) (Jiang *et al.* 2018)

Test Frame	Column	Middle bay beam	Side bay beam
Frame 1	$50 \times 30 \times 3$	$150 \times 50 \times 5$	$60 \times 40 \times 3.5$
Frame 2	$50 \times 30 \times 3$	$60 \times 40 \times 3.5$	$60 \times 40 \times 3.5$

Table 2 Gravity loads applied to the test frames (Jiang *et al.* 2018)

Test Frame	m_1 (N)	m_2 (N)	m_3 (N)	m_4 (N)	m_5 (N)	m_6 (N)
Frame 1	2910.0	1760.7	701.3	766.0	73.9	74.0
Frame 2	4667.3	2312.4	751.1	766.0	69.7	81.7

2.5 Collapse assessment

Assessment of whether the structure could sustain the fire is made based on the comparison of the maximum allowable displacement ($U_{i,allow}^{u}$) obtained in step (3) and the maximum displacement ($U_{i,max}^{h}$) obtained in the nonlinear dynamic analysis in step (4). If $U_{i,max}^{h} \leq U_{i,allow}^{u}$, progressive collapse will not occur, otherwise, progressive collapse is considered to occur.

3. Validation

Test results of two planar steel frames (Frames 1 and 2) under localized furnace loading, which were conducted by Jiang *et al*. (2018), were employed to validate the proposed progressive collapse resistance assessment method. The tests explicitly considered dynamic effect of structural performance under thermal loading.

3.1 Brief description of the test frames

The frame dimensions and the test set-up are illustrated in Fig. 5. As shown in Fig. 5, the test steel frames contained four bays and two storeys. Sections of the beams and columns of both test frames were rectangular tubes, details of which are presented in Table 1. The beam-to-column connections were welded connections. Triangular steel plates with dimension of $50 \times 30 \times 3$ (mm) were used to stiffen the connections to prevent failure of the connections. Gravity loads were applied to load the test frames, and the middle column at the first storey was heated by an electrical furnace. Details of the applied gravity loads are presented in Table 2. Materials of the columns and beams were steel 20 (GB/T8162 2008) and that of the stiffeners was steel Q345 (GB/T1591 2008), which are structural steels made in China. Mechanical properties of these two types of steel Gas temperature of the furnace, frame temperature, displacements and strains at certain locations of the test frames were measured. More details of the test frames could be referred to the literatures (Jiang *et al*. 2017, Jiang *et al.* 2018).

3.2 Numerical modelling

This subsection introduces the modelling techniques used in the finite element analysis of this manuscript. However, it is important to note that the software and modelling techniques used in this study are not the requirements of GLAM. All capable software programs and rational modelling techniques could be used by GLAM.

The model of the heated column was built using the software ABAQUS (Dassault Systemes Simulia Corp 2014). Beam element (B31) is used to model the beams and columns. The element B31 is a three-dimensional Timoshenko beam element which is capable of modelling axial, shear and flexure deformation of beams or columns.

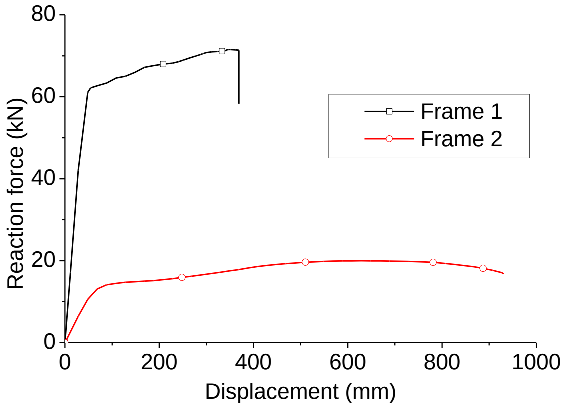

Fig. 6 Reaction force-displacement curves of the equivalent axial restraints (k_{lteq}) of Frames 1 and 2

Each beam is modelled with 24 elements and each column 20 elements, with the size of the elements being around 250 mm and 180 mm, respectively. The adopted mesh sizes are small enough for the analysis as already demonstrated in literature (Jiang *et al.* 2015). For the heated column, an initial imperfection is assumed as sine curve shape with a maximum deflection of 1/1000 of the column length. The stiffened parts of the beams and columns near the beam-to-column connections were modelled by amplifying the section height by 50 mm which equals to the edge length of the triangular stiffeners. Shared point is used at each intersection point of the beams and columns to model the rigid beam-to-column connection. Each restraint spring at boundary of the heated column is modelled with a spatial connection element (CONN3D2), which could be used to connect two nodes or ground and a node. The curve of reaction force against displacement of the connection element could be defined by the user, and nonlinear behaviour could be considered by this element. Nonlinear explicit dynamic method is adopted for this analysis, and time scale technique is used to model the process of thermal loading. In the explicit dynamic analysis of the studied cases, the heating process is scaled down to 30 seconds. Validation of the adopted time scale technique has been presented in the literature (Jiang *et al.* 2015).

Temperature of the heated column of each steel frame was adopted as the same with that that suggested in literature (Jiang *et al.* 2017). Namely, temperature of the lower 1.02 m part of the heated column were assumed to be uniform, while that between the height of 1.02 m to the column top was assumed to be linearly distributed along the height with the column top has a lower temperature.

Elastic-plastic material model was adopted for steel. Material properties of the tested frames were adopted as the measured values from coupon tests, and temperature distributions of the heated components were adopted according to the temperature measurement of the tests (Jiang *et al.* 2018). The Cowper-Symonds model (Cowper and Symonds 1957) is adopted to consider the effect of strain rate on yield strength of steel with the following equation

$$\sigma_{yd}/\sigma_y = 1 + \left(\frac{\dot{\varepsilon}}{C}\right)^{\frac{1}{P}} \tag{3}$$

where σ_{yd} is the dynamic yield strength; σ_y is the static yield strength; $\dot{\varepsilon}$ is the strain rate; C and P are material parameters. Values for parameters C and P are taken to be 40.4 /s and 5 respectively, according to the suggestion in the research literature (Al-Thairy and Wang 2011).

3.3 Results of GLAM and comparison with test results

The reaction-displacement curves of the equivalent springs (k_{lteq}) of the Frames 1 and 2 are presented in Fig. 6. As shown in Fig. 6, the reaction force reached the peak value of 71.52 kN at displacement of 351 mm for Frame 1, and 19.98 kN at displacement of 629 mm for Frame 2. The reaction forces declined with further increase of the displacement, because after this point, the adjacent column started to fail. Therefore, the maximum allowable vertical displacement of Frames 1 and 2 are 351 mm and 629 mm, respectively. The curves of vertical displacement at top of the heated column against the column temperature obtained from GLAM are presented in Fig. 7, in which also presented the test results. It can be seen from Fig. 7, according to GLAM, the maximum vertical displacement of Frames 1 and 2 are 5.3 mm and 70.7 mm, respectively, both of which are less than the maximum allowable vertical displacements. Hence, according to the assessment results of GLAM, progressive collapse would not occur to both frames. This prediction is supported by the test results (Jiang *et al*. 2018).

As can also be seen from Fig. 7, the curves obtained from GLAM agree well with test results. It is noted that in the test of Frame 2, the displacement continued to increase in the temperature range of around 750°C to 800°C in the test. This is because after the large deformation of Frame 2, hot gas in the furnace escaped, heating and softening the beams connected to the heated column, as explained in literature (Jiang *et al*. 2017). It is also noted in the analysis results of Frame 2 that there are some vibrations of the displacement after the heated column buckled due to dynamic effects, while the displacement of the test curve continued to increase with no vibration. This may also because of the heating and softening of the beam connected to the heated column caused by the escaped hot gas from the furnace.

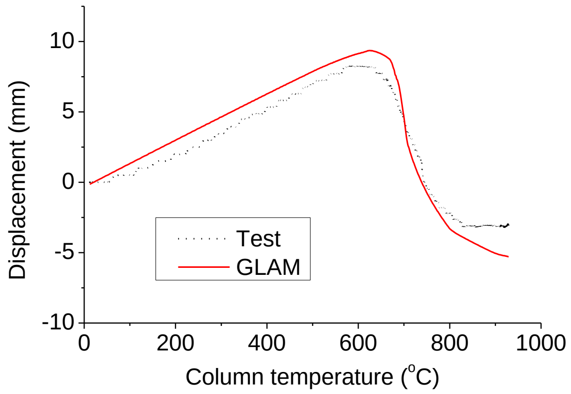

(a) Frame 1

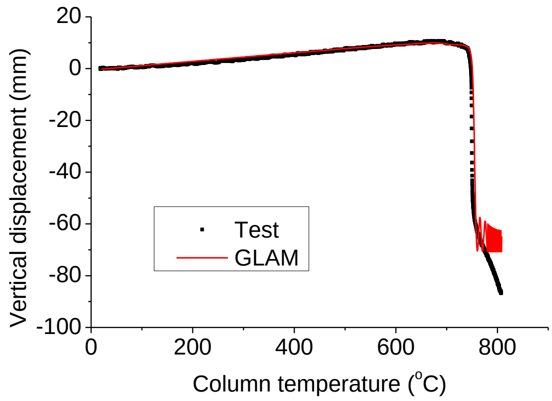

(b) Frame 2

Fig. 7 Results comparison between GLAM and the tests on vertical displacement at top of the heated column against temperature of this column

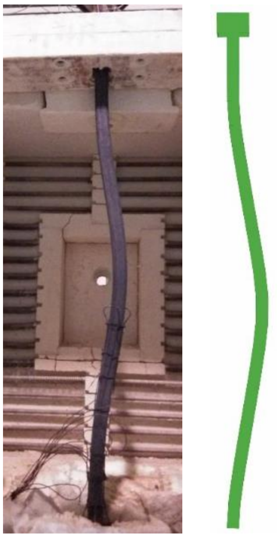

(a) Frame 1

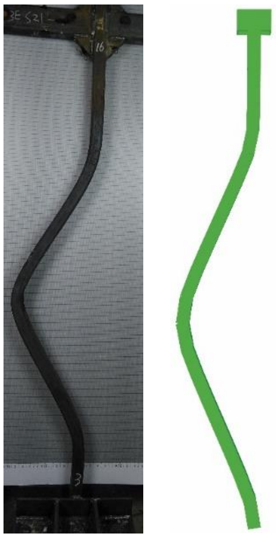

(b) Frame 2

Fig. 8 Comparisons of frame deformation shapes obtained from test and analysis

Fig. 8 shows the comparisons of frame deformation shapes obtained from test and analysis. It can be seen from the figures that the failure mode of the heated column and deformation shape of the heated column obtained from GLAM are concordant with test results. As shown in Fig. 8, the maximum lateral deflection points of the heated column of the both test frames were located at around mid-height of the column, but slightly closer to the lower end. It should be noted in the test photo shown in Fig. 8(a) that around 200 mm height of the column near the column top was hidden in insulation material, which may makes the column in the photo visually seems shorter. It is noted that for the deformation shapes of the heated column at the column foot, there are some differences between the test results and analysis results for both test frames. The reason is that in the analysis, the temperature at the column foot was assumed to be the same as that at column middle as suggested in literature (Jiang *et al.* 2017). However, in the test, because heated will be transferred away from the column foot to the base, the temperature at the column foot is slightly lower than that at the column middle as reported in (Jiang *et al.* 2018). Hence, the point of inflection in the analysis results at the column foot is slightly lower than that in the test results.

4. Examples of a 2D steel frame

4.1 The steel frame for case studies

A planar steel frame designed in a published paper (Jiang *et al.* 2015), as shown in Fig. 9, is employed as an example to illustrate the application of GLAM on 2D steel frames. The designed planar steel frame is an ordinary moment resistant frame which is commonly used in seismic zones like East Asia. The frame contains 6 storeys and 4 bays, the height of each storey is 3.6 m and the span of each bay is 6 m. Uniform H sections are adopted for the columns

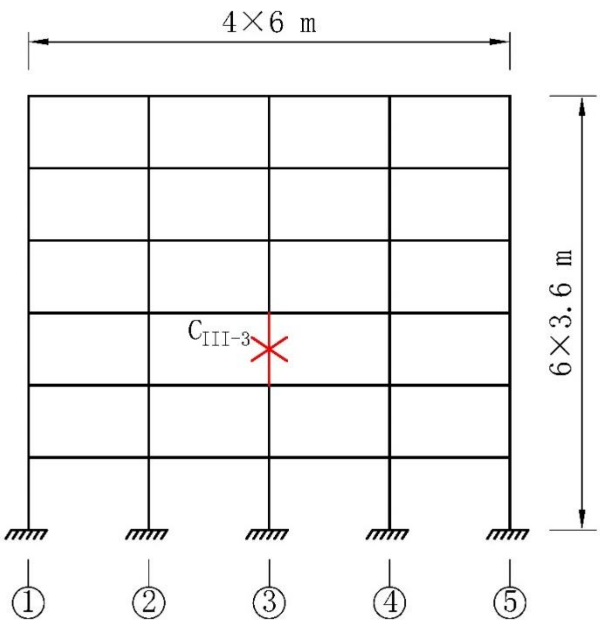

Fig. 9 Reference steel frame with one column fails in fire

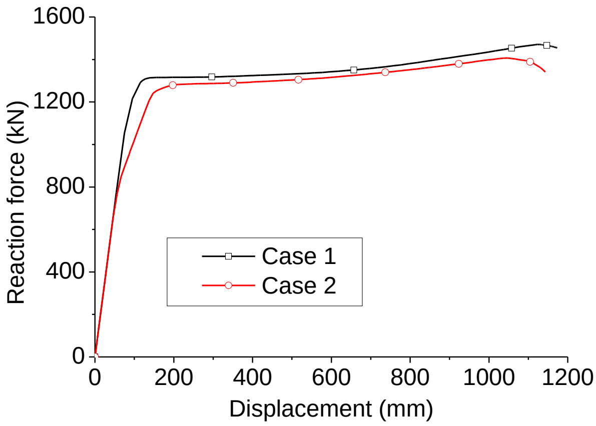

Fig. 10 Reaction force-displacement curves of the equivalent axial restraints (k_{lteq}) in Cases 1 and 2

and beams respectively and the columns are oriented to bend about their minor axes. The section of the columns is $HW350 \times 350 \times 12 \times 19$ (mm) and that of the beams is $HW340 \times 250 \times 9 \times 14$ (mm). The beam-to-column connections are welded rigid connections. The column C_{III-3} is considered to be the heated column, as shown in Fig. 9. The temperature of the heated column could be obtained through detailed thermal analysis. It is worth noting that fire protection is normally designed for steel building structures, which could be considered through the thermal analysis. Since these case studies are mainly aimed at illustrating the application of the GLAM, the heated column (C_{III-3}) is assumed to be uniformly heated from ambient temperature 20ºC to 1200ºC. Q345 Steel is adopted for the structural components. The steel properties at ambient temperature are taken to be elastic-perfectly plastic, with yield strength of 345 N/mm^2 and elastic modulus of 2.1×10^5 N/mm^2. For steel properties at elevated temperatures, the stress-strain relationship proposed in Eurocode 3 Part 1.2 (BS EN 1993-1-2 2005) is adopted. The thermal expansion of steel is taken to be a constant value of 1.4×10^{-5}/ºC. Uniform vertical load p is applied to the beams. Two cases with different load levels are considered: Case 1 with p = 35 kN/m and Case 2 with p = 80 kN/m, which represent a relatively low load level and a high load level for the reference frame, respectively.

4.2 Assessment procedure and results

The internal compressive axial forces of the heated column (C_{III-3}) at ambient temperature in Case 1 and Case 2 are 840.29 kN and 1919.67 kN respectively. The vertical downward displacements at the bottom point of column C_{III-3} in Case 1 and Case 2 are 2.32 mm and 5.36 mm, respectively. For both case studies, the axial stiffness of the heated column is 9.94×10^8 N/m and the rotational stiffness of the heated column is 3.17×10^7 N•m.

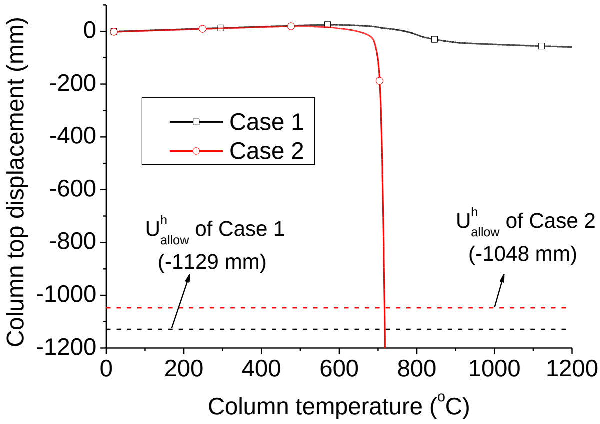

Fig. 11 Vertical displacement at top of the heated column against temperature of this column in Cases 1 and 2

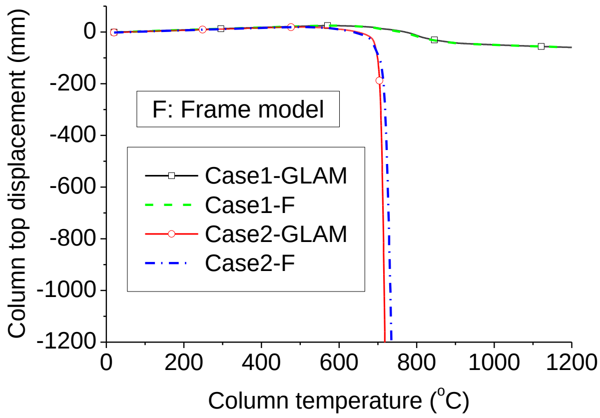

Fig. 12 Results comparison between GLAM and whole frame model analysis on vertical displacement at top of the heated column against column temperature in Cases 1 and 2

The reaction-displacement curves of the equivalent springs (k_{lteq}) of the Cases 1 and 2 are shown in Fig. 10. It can be seen from Fig. 10 that for Case 1, the restraint stiffness in the vertical displacement range from 0 to 75 mm is almost constant, and when that displacement passes around 120 mm the reaction force increases gradually with the increase of displacement. The reaction force reaches the maximum value at around 1129 mm and then starts to decline with the further increase of displacement. This is because that the adjacent columns of the heated column buckled at this displacement. Therefore, progressive collapse will occur in Case 1 when the vertical displacement reaches 1129 mm. Similarly, the critical vertical displacement of progressive collapse of Case 2 is around 1048 mm. It is worth noting in Fig. 10 that the spring in Case 2 reaches non-linear stage earlier than that of Case 1. Besides, the ultimate strength of the equivalent spring in Case 2 is also smaller than that of Case 1. This shows that the value of the applied load has significant influence on the reaction-displacement curve of the equivalent spring (k_{lteq}) of the heated column. Since the upward displacement of the heated column under fire is small, the upward restraint at column top remains elastic and the upward restraint stiffness is the same with that of downward restraint.

Nonlinear dynamic analysis of the heated column model was conducted for each studied case. The obtained curves of vertical displacement at top of the heated column against column temperature of the case studies are shown in Fig. 11, in which the maximum allowable vertical displacement at top of the heated column for each case is also presented. As shown in Fig. 11, the heated column in Case 1 fails gradually, and the maximum vertical displacements at the column top is around 59 mm. In contrast, the heated column in Case 2 fails dynamically. Besides, the buckling temperature of the heated column in Case 2 is lower than that in Case 1. The collapse assessment for each studied case is made through comparison of the maximum allowable displacement and the largest displacement of the heated column. As can be seen from Fig. 11, the frame in Case 1 will not collapse while that in Case 2 will collapse.

4.3. Compared with results of whole structure model

Nonlinear dynamic analyses were conducted to study the performance of the whole frame of the case studies for comparison. The finite element model of the whole frame was also built by using the software ABAQUS, and the analysis method used in the whole structure model is the same as that in the aforementioned heated column model.

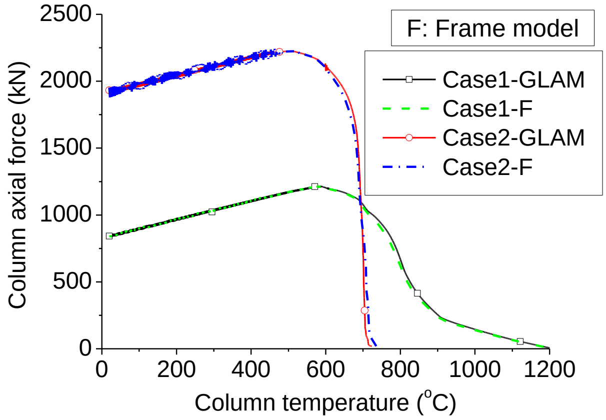

Fig. 13 Results comparison between GLAM and whole frame model analysis on compressive axial force of the heated column against temperature of this column

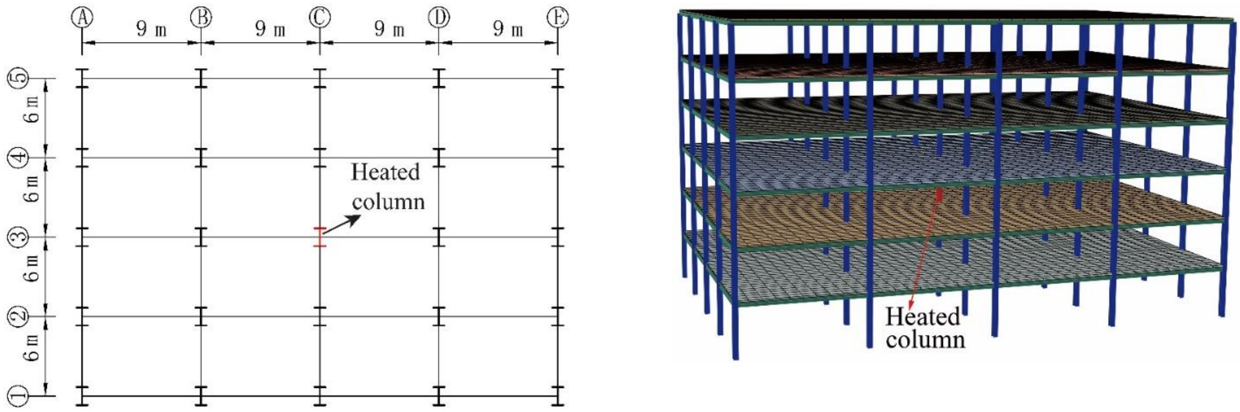

(a) Plan view (b) Numerical model

Fig. 14 Reference 3D Steel framed structure with one column fails in fire

Comparisons on vertical displacement at top of the heated column between the results obtained from analysis of the whole frame model and those from the GLAM were made as shown in Fig. 12. It can be seen from Fig. 12 that the two displacement-temperature curves of Case 1, which were obtained from GLAM and analysis of the whole frame model respectively, are almost coincide with each other. Besides, the differences on the failure temperature of the frame in Case 2, which is defined as the temperature at which the vertical displacement at top of the heated column reaches the maximum allowable displacement, between GLAM and analysis of the whole frame model are within 20 ºC. It is noted that the failure temperatures predicted by GLAM are slightly lower than those obtained from analysis of the whole frame model. Fig. 13 presents comparisons on the axial forces in the heated column between GLAM and analysis of the whole frame model. It can be seen from Fig. 13 that the curves of axial force in the heated column obtained from GLAM and analysis of the whole frame model also match well with each other for both case studies.

5. Example of a 3D steel frame with concrete slabs

5.1 The steel frame for case studies

Application of GLAM on 3D Steel framed structures is also presented through a case study. Fig. 14 shows a 3D steel framed structure with one column fails in fire. As shown in Fig. 14, the considered 3D steel frame has four bays of 9 m, four bays of 6 m, and six storeys of 3.6 m. The section of all the columns is HW$350 \times 350 \times 12 \times 19$ (mm) and that of the beams is HW$294 \times 200 \times 8 \times 12$ (mm). The beam-to-column connections are welded rigid connections. The concrete slabs have a thickness of 120 mm, and are reinforced by steel bars with a diameter of 10 mm and in spacing of 200 mm. The net thickness of the concrete cover of the steel bars is 20 mm. Material of the steel columns and beams is Q345, which is the same with the 2D steel frame in Cases 1 and 2. Material of the concrete slab is C30 with a compressive strength of 33 MPa and a tensile strength of 2.6 MPa, and an elastic modulus of 3.1×10^4 MPa. Material of the reinforcement steel bars was HPB 400, which has a yield strength of 400 MPa and an elastic modulus of 2.0×10^5 MPa. The concrete damaged plasticity model was adopted to model the concrete material. One inner column is considered to be heated as shown in Fig. 14. A uniform distributed load of 6 kN/m^2 was applied to the slabs. The concrete slabs were modelled by four-node shell elements with reduced integration (S4R) in a mesh size of 0.6 m $\times$ 0.9 m, as shown in Fig. 14(b). Each layer

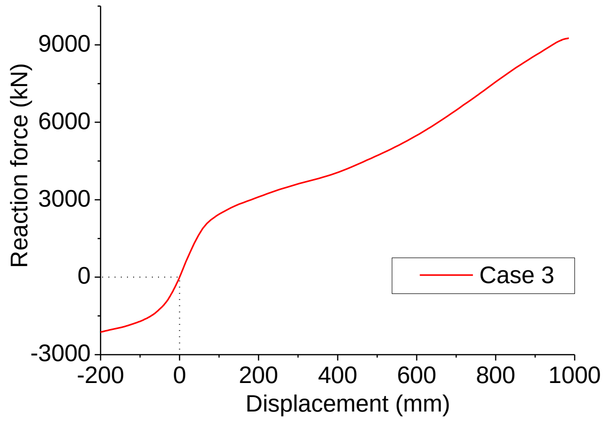

Fig. 15 Reaction force-displacement curve of the equivalent axial restraints (k_{lteq}) for Cases 3

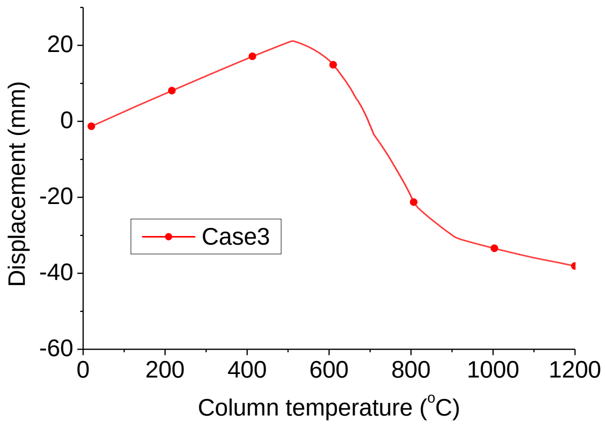

Fig. 16 Vertical displacement at top of the heated column against temperature of this column in Cases 3

of reinforcements in the concrete slab was considered by defining a "rebar layer" in the concrete slab. The "tie" constraint was used between the beams and the concrete slabs to model the composite response of the composite slabs. Modelling method of the steel frame was the same with that of the 2D steel frame.

5.2 Assessment procedures and results

The internal compressive axial forces of the heated column at ambient temperature in Case 3 was 1296.55 kN. The vertical downward displacements at the bottom point of the heated column in Case 3 is 3.58 mm respectively. The axial stiffness and rotational stiffness of the heated column is 9.94×10^8 N/m and 3.17×10^7 N•m, respectively.

Fig. 15 shows the reaction-displacement curve of the equivalent springs (k_{lteq}) of Case 3. It is worth noting that due to the existence of the concrete slab, the reaction-displacement curves of upward and downward were not symmetrical. Besides, when the downward displacement reached round 985 mm, failure occurred to the concrete slabs. Hence, the maximum allowable displacement was around 985 mm. Since the upward displacement of the heated column top is normally small, the upward reaction-displacement curve was only presented to the displacement of 200 mm.

Nonlinear dynamic analysis was conducted to the column model to obtain the performance of the heated column. The curve of vertical displacement at top of the heated column against column temperature of Case 3 is shown in Fig. 16. As can be seen in Fig. 16, the maximum vertical displacement at top of the heated column is around 38 mm which is less than the maximum allowable displacement. Hence, the 3D steel frame in Case 3 will not collapse.

5.3 Compared with results of whole structure model

Nonlinear dynamic analysis of the whole structure model was also conducted in Case 3 for comparison. Fig. 17 shows the comparisons on vertical displacement at top of the heated column between the results obtained from analysis of the whole frame model and those from GLAM. It can be seen from Fig. 17 that the two displacement-temperature curves of Case 3 are almost coincide with each other. Fig. 18 presents comparison on the axial forces in the heated column between GLAM and analysis of the whole frame model. As can be seen from Fig. 18, GLAM also gives reasonable results to the axial force of the heated column.

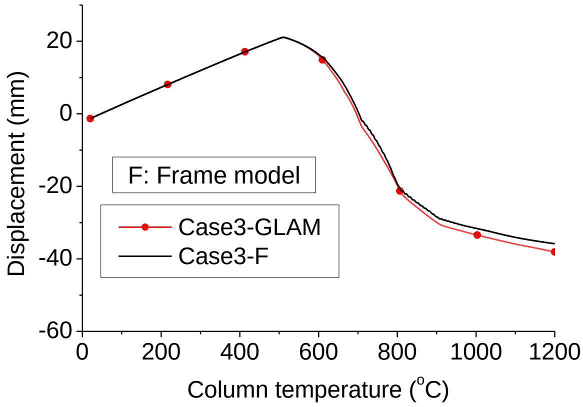

Fig. 17 Results comparison between GLAM and whole frame model analysis on vertical displacement at top of the heated column against column temperature in Cases 3

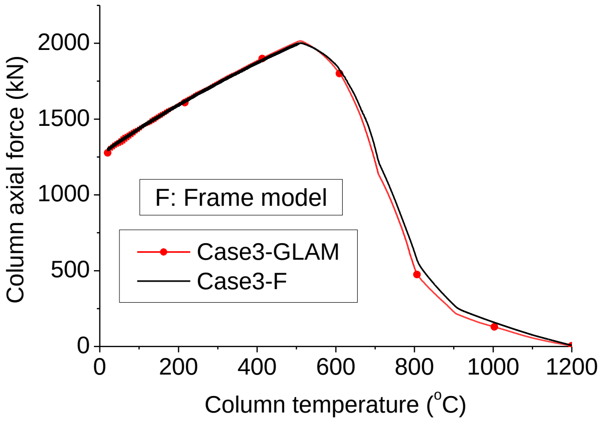

Fig. 18 Results comparison between GLAM and whole frame model analysis on compressive axial force of the heated column against column temperature in Case 3

Table 3 Comparison of CPU time costed by analysis of the heated column model (t_{GLAM}) and that of whole frame model (t_{Frame})

Case	t_{GLAM} (min)	t_{Frame} (min)	(t_{Frame}- t_{GLAM})/ T_{Frame}
Case 1	8.5	29.5	71%
Case 2	5.5	18.5	69%
		Average	70%
Case 3	9.5	809.5	99%

6. Discussion

6.1 Efficiency of GLAM

To identify the efficiency of the proposed method, the CPU time cost by completing the explicit dynamic analyses of the heated column model and the whole frame model in all the case studies was monitored, as listed in Table 3. All the analyses were conducted in the same computer with the same result output frequency. As shown in Table 3, by adopting GLAM, around 70% CPU time was saved for the studied 2D steel frame, and 99% CPU time was saved for the studied 3D steel frame. It is noted that the time cost by both GLAM and nonlinear dynamic analysis of the whole frame mode in Case 2 is shorter than that in Case 1, because the analyses in Case 2 were aborted after progressive collapse occurred as can be seen in Fig. 12. It is also noted that the time cost by nonlinear dynamic analysis of the whole frame model of the 3D steel frame (Case 3) was much longer than that of 2D steel frame (Cases 1 and 2). That is because the 3D steel frame has significantly more structural components than the 2D steel frame. On the other hand, the time cost by GLAM in Case 3 is only slightly longer than that in Case 1, because the amounts of elements of the column model in Case 3 and Case 1 were the same. Therefore, for a 3D steel structure with more storeys or more bays than the studied case, the efficiency of adopting GLAM will be even higher. It is noted that the time needed

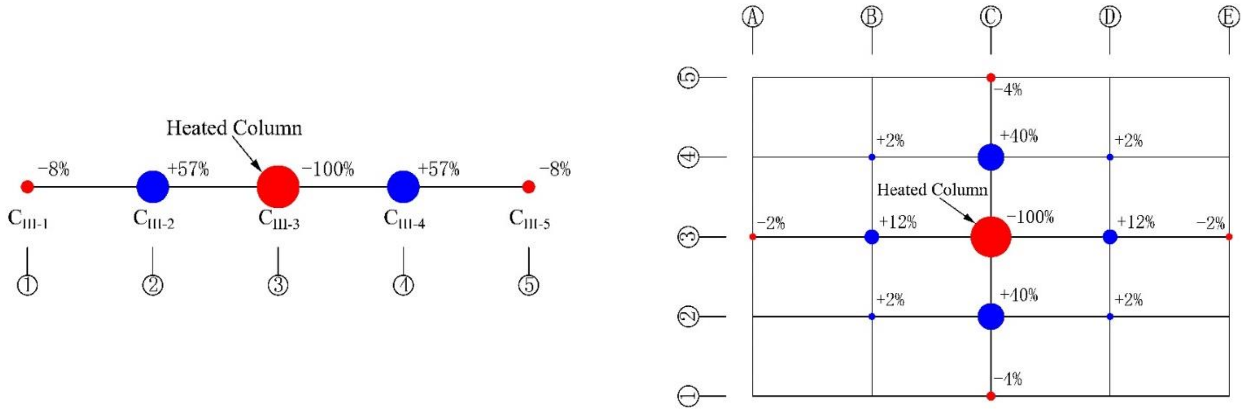

(a) Case 1 - 2D steel frame

(b) Case 3 - 3D steel frame with concrete slabs

Fig. 19 Load redistribution when one column fails under fire

to build the numerical models in adopting GLAM and that to build the whole structure model may be different. Since it is difficult to give objective estimations on the time needed to build a numerical model, the time needed to build the models is not compared in the current study.

6.2 Load redistribution

After failure of the heated column, load redistribution will occur in the structure. Case 1 and Case 3 are adopted as examples of 2D steel frames and 3D steel frames, respectively, to illustrate this load redistribution. Fig. 19 illustrates the variation of axial force among the columns in the same storey of the heated column, as a ratio of axial force change in each column to the axial force of the heated column at ambient temperature. As can be seen in Fig. 19(a), when the heated column in the planar steel frame fails in fire, the load carried by this column was mainly redistributed to the adjacent columns at both sides, the increase of axial force of which is 57%. When the heated column of the 3D steel frame in Case 3 failed, the load carried by it was also mainly redistributed to the adjacent columns. However, the maximum increase of axial force in the adjacent columns in a 3D steel frame is around 40%, which is significantly lower than that in a 2D steel frame. That is because load can be redistributed to two vertical directions in a 3D steel frame as shown in Fig. 19(b), instead of only one direction in 2D steel frames. Besides, the increase of axial force in the adjacent columns in the direction with a shorter span of 6 m is significantly larger than that with a longer span of 9 m.

7. Conclusions

This paper proposes a simplified robustness assessment method entitled Global-Local Analysis Method (GLAM) for multi-storey steel framed structures under fire-induced column failure. The GLAM combines nonlinear dynamic analysis of the heated column and static analysis of the overall structure excluding the heated column to assess the progressive collapse of multi-storey steel frame structure, as shown in the following five steps: (1) calculation of response of the structure under design load; (2) analysis of nonlinear static response of the unheated sub-structure; (3) determination of maximum allowable deflection of the unheated sub-structure; (4) analysis of nonlinear dynamic response of the heated column; and (5) assessment of progressive collapse.

Test results of two steel frames under localized fire, which considered dynamic effect of column buckling, were used to validate the proposed GLAM. Results show that the GLAM gives reasonable results to the performance of the test frames.

Several case studies of a 2D steel frame and a 3D steel frame with concrete slab were conducted to illustrate the application of GLAM. Comparison between the results obtained from GLAM and those from nonlinear dynamic analyses of the whole structure model was also made to illustrate the accuracy and efficiency of GLAM. The results predicted by GLAM were concordant with those obtained from the dynamic nonlinear analysis of the whole structure model for both the cases of 2D steel frame and the case of 3D steel frame. It is noted that compared with dynamic nonlinear analysis of the whole structure model, around 70% CPU time was saved on average for the studied cases of the 2D steel frame by GLAM, and 99% CPU time was saved for the case of 3D steel frame, illustrating that GLAM is much more computationally efficient.

Results of the case studies also show that the value of load applied to the frame has notable effects on the restraints offered by the unheated sub-structure to the heated components. Hence, when determining the restraint condition of a heated structural component in a structure for robustness assessment, the load level of the structure is suggested to be considered. Besides, compared with 2D steel frames, 3D steel frames have more load transfer paths when one column fails, and the increase of axial load in the adjacent column of the heated column, as a percentage of axial force of the heated column at ambient temperature, is significantly smaller than that in 2D steel frames. Moreover, in a 3D steel frame structure, the increase of axial force in the adjacent columns in the direction with a shorter span is significantly larger than that with a longer span.

The meaning of the proposed GLAM is that it offers an efficient and effective method to assess the progressive collapse of either two-dimensional (2D) steel frames or three-dimensional (3D) steel frames with concrete slabs under fire-induced column failure. GLAM simplifies the assessment process by avoiding the time consuming nonlinear dynamic analysis of the whole structure, but at the same time reflects key features of the structural performance. Further development of the GLAM includes extensive experimental validations and application of the GLAM to different kinds of structures.

Acknowledgements

This work was supported by the National Natural Science Fundation of China with Grant No. 51908560, No. 51120185001 and Ministry of Science and Technology of China with Grant No. SLDRCE14-A-05.

References

Agarwal, A. and Varma, A.H. (2014), “Fire induced progressive collapse of steel building structures: the role of interior gravity columns”, *Eng. Struct*., **58**, 129-140. https://doi.org/10.1016/j.engstruct.2013.09.020.

Al-Thairy, H. and Wang, Y.C. (2011), “A numerical study of the behaviour and failure modes of axially compressed steel columns subjected to transverse impact”, *Int. J. Impact Eng*., **38**(8-9), 732-744. https://doi.org/10.1016/j.ijimpeng.2011.03.005.

BS EN 1993-1-2 (2005), *Eurocode 3: Design of steel structures Part 1-2: General rules - Structural fire design*, European Committee for Standardization , Brussels.

Cowper, G.R. and Symonds, P.S. (1957), *Strain-Hardening and Strain-Rate Effects in the Impact Loading of Cantilever Beams*, Report, Brown University, Providence, Rhode Island, USA

Dassault Systemes Simulia Corp (2014), *Getting Started with ABAQUS Interactive Edition, Verson 6.14-4*,

Ellingwood, B.R. and Dusenberry, D.O. (2005), “Building design for abnormal loads and progressive collapse”, *Comput. - Aided Civ. Inf.*, **20**(3), 194-205.

El-Tawil, S., Li, H. and Kunnath, S. (2014), “Computational simulation of gravity-induced progressive collapse of steel-frame buildings: current trends and future research needs”, *J Strcut. Eng*., **140**(8SI). https://doi.org/10.1061/(ASCE)ST.1943-541X.0000897.

Fang, C., Izzuddin, B.A., EIghazouli, A.Y. and Nethercot, D.A. (2011), “Robustness of steel-composite building structures subject to localised fire”, *Fire Safety J.*, **46**(6), 348-363. https://doi.org/10.1016/j.firesaf.2011.06.001.

Fang, C., Izzuddin, B.A., Elghazouli, A.Y. and Nethercot, D.A. (2013), “Simplified energy-based robustness assessment for steel-composite car parks under vehicle fire”, *Eng. Struct*.,**49**, 719-732. https://doi.org/10.1016/j.engstruct.2012.12.036.

Ferraioli, M. (2019), “Evaluation of dynamic increase factor in progressive collapse analysis of steel frame structures considering catenary action”, *Steel Compos. Struct.*, **30**(3), 253-269. https://doi.org/10.12989/scs.2019.30.3.253.

GB/T8162 (2008), *Seamless steel tubes for structural purpose*, Standardization Administration of the People's Republic of China, Beijing, China.

GB/T1591 (2008), *High strength low alloy structural steels*, Standardization Administration of the People's Republic of China, Beijing, China.

Grierson, D.E., Xu, L. and Liu, Y. (2005), “Progressive-failure analysis of buildings subjected to abnormal loading”, *Comput. - Aided Civ. Inf.*, **20**(3), 155-171. https://doi.org/10.1111/j.1467-8667.2005.00384.x.

Izzuddin, B.A., Vlassis, A.G., Elghazouli, A.Y. and Nethercot, D.A. (2008), “Progressive collapse of multi-storey buildings due to sudden column loss - Part I: Simplified assessment framework”, *Eng. Struct*., **30**(5), 1308-1318. https://doi.org/10.1016/j.engstruct.2007.07.011.

Jiang, B., Li, G. and Usmani, A. (2015), “Progressive collapse mechanisms investigation of planar steel moment frames under localized fire”, *J. Contr. Steel Res*., **115**, 160-168. https://doi.org/10.1016/j.jcsr.2015.08.015.

Jiang, B., Li, G., Li, L. and Izzuddin, B.A. (2017), “Simulations on progressive collapse resistance of steel moment frames under localized fire”, *J. Contr. Steel Res*., **138**, 380-388. https://doi.org/10.1016/j.jcsr.2017.05.018

Jiang, B., Li, G., Li, L. and Izzuddin, B.A. (2018), “Experimental Studies on Progressive Collapse Resistance of Steel Moment Frames under Localized Furnace Loading”, *J. Struct. Eng.*, **144**(2). https://doi.org/10.1061/(ASCE)ST.1943-541X.0001947.

Jiang, B., Li, G.Q. and Izzuddin, B.A. (2016), “Dynamic performance of axially and rotationally restrained steel columns under fire”, *J. Contr. Steel Res*., **122**, 308-315. https://doi.org/10.1016/j.jcsr.2016.03.013.

Jiang, J. and Li, G. (2017), “Progressive collapse analysis of 3D steel frames with concrete slabs exposed to localized fire”, *Eng. Struct*., **149**, 21-34. https://doi.org/10.1016/j.engstruct.2016.07.041.

Kim, J. and Park, J. (2008), “Design of steel moment frames considering progressive collapse”, *Steel Compos. Struct.*, **8**(1), 85-98. https://doi.org/10.12989/scs.2008.8.1.085.

Kwon, I. and Kwon, Y. (2012), “Determination of limiting temperatures for H-section and hollow section columns”, *Steel Compos. Struct.*, **13**(4), 309-325. https://doi.org/10.12989/scs.2012.13.4.309.

Lange, D., Roeben, C. and Usmani, A. (2012), “Tall building collapse mechanisms initiated by fire: Mechanisms and design methodology”, *Eng. Struct*., **36**, 90-103.

Lew, H.S., Bukowski, R.W. and Carino, N.K. (2005), *Federal Building and Fire Safety Investigation of the World Trade Center Disaste*r, Report, NIST, USA

Marjanishvili, M.S. (2004), “Progressive analysis procedure for progressive collapse”, *J. Perform Constr. Fac*., **2**(18), 79-85. https://doi.org/10.1061/(ASCE)0887-3828(2004)18:2(79).

Mashhadi, J. and Saffari, H. (2017), “Dynamic increase factor based on residual strength to assess progressive collapse”, *Steel Compos. Struct.*, **25**(5), 617-624. https://doi.org/10.12989/scs.2017.25.5.617.

Pearson, C. and Delatte, N. (2005), “Ronan point apartment tower collapse and its effect on building codes”, *J. Perform Constr. Fac*., **19**(2), 172-177. https://doi.org/10.1061/(ASCE)0887-3828(2005)19:2(172).

Rackauskaite, E., Kotsovinos, P. and Rein, G. (2017), “Model parameter sensitivity and benchmarking of the explicit dynamic solver of LS-DYNA for structural analysis in case of fire”, *Fire Safety J.*, **90**, 123-138. https://doi.org/10.1016/j.firesaf.2017.03.002.

Renaud, C., Aribert, J.M. and Zhao, B. (2003), “Advanced numerical model for the fire behaviour of composite columns with hollow steel section”, *Steel Compos. Struct.*, **3**(2), 75-95. https://doi.org/10.12989/scs.2003.3.2.075.

Sasani, M. and Kropelnicki, J. (2008), “Progressive collapse analysis of an RC structure”, *Struct. Des Tall Spec.*, **17**(4), 757-771. https://doi.org/10.1002/tal.375.

Sun, R., Huang, Z. and Burgess, I.W. (2012), “Progressive

collapse analysis of steel structures under fire conditions", *Eng. Struct.*, **34**, 400-413. https://doi.org/10.1016/j.engstruct.2011.10.009.
Usmani, A.S., Chung, Y.C. and Torero, J.L. (2003), "How did the WTC towers collapse: a new theory", *Fire Safety J.*, **38**(6), 501-533. https://doi.org/10.1016/S0379-7112(03)00069-9.
Wald, F., Chladna, M., Moore, D., Santiago, A. and Lennon, T. (2006), "Temperature distribution in a full-scale steel framed building subject to a natural fire", *Steel Compos. Struct.*, **6**(2), 159-182. https://doi.org/10.12989/scs.2006.6.2.159.

DL